ISSN 1063-7729, Astronomy Reports, 2020, Vol. 64, No. 8, pp. 693–710. © Pleiades Publishing, Ltd., 2020.
Russian Text © The Author(s), 2020, published in Astronomicheskii Zhurnal, 2020, Vol. 97, No. 8, pp. 664–682.

# Impact of the Small-Scale Spatial Distribution of Dust Particles on the Chemical Evolution of the Diffuse Interstellar Medium

**V. A. Sokolova[a, b, *], A. I. Vasyunin[a, b, **], A. B. Ostrovskii[a, ***], and S. Yu. Parfenov[a, ****]**

[a] *Ural Federal University, Yekaterinburg, Russia*
[b] *Ventspils University College, VIRAC, Ventspils, Latvia*
**e-mail: valeria.sokolova@urfu.ru*
***e-mail: anton.vasyunin@urfu.ru*
****e-mail: andrey.ostrovsky@urfu.ru*
*****e-mail: sergey.parfenov@urfu.ru*

Received March 26, 2020; revised March 30, 2020; accepted March 30, 2020

**Abstract**—In this work we analyze the effect of gas-dust clumps, possibly formed in the interstellar medium due to instability, described in [10], on the chemical evolution of the diffuse interstellar medium. For this purpose we calculate chemical evolution with common parameters of diffuse interstellar medium (ISM). It is shown that abundances of most observed molecules are higher in a model of the diffuse medium with clumps than in a model with homogeneous dust distribution. In some cases it leads to better agreement of modelling abundances and their relations with observational data. But at the same time, it does not mean that the hypothesis about inhomogenous dust distribution can qualitatively improve the agreement between modelling and observational data on the chemical composition of the diffuse interstellar medium. The best-fit range of values of the physical characteristics of the medium is wider under the assumption that dust can form compact gas-dust clumps and is not uniformly mixed with gas. Results described in this work show that small-scale (≤1 au) inhomogeneities of the interstellar medium can be important for its chemical evolution.

**DOI:** 10.1134/S1063772920090061

## 1. INTRODUCTION

Diffuse atomic and molecular clouds are of great interest in studies of the interstellar medium. It is believed that they represent an intermediate stage in formation of cold dense clouds and further stages of star formation [1, 2].

The diffuse interstellar clouds are characterized by low gas temperatures (30–100 K) and relatively low gas densities (10–500 $cm^{-3}$) (see Table 1 in [3]). These clouds have a visual extinction $\leq 1^m$ and are thus quite transparent to the ambient interstellar radiation. The analysis of diffuse cloud observations can be complicated due to confusion arising when a studied line-of-sight crosses a number of the diffuse clouds or a mixture of different types of clouds. As a result, modern knowledge of the physical and chemical processes in the diffuse clouds is incomplete.

According to observations, the abundances of a number of molecular species in the diffuse clouds exceed those predicted by models of diffuse clouds and are more consistent with ones in dense molecular clouds (see, for example, [4–9] and others). These high abundances are unexpected in the diffuse clouds where the interstellar radiation field plays a large role in the chemical processes and dissociates molecules efficiently.

Therefore, the models, which traditionally assume homogeneous gas and dust spatial distribution, encounter a number of difficulties in reproducing the observed molecular abundances. However, it was recently shown that there is a previously unknown specialtype of instability (ion shielding or "ion shadowing force") which occurs in both diffuse and dense cloud conditions in the presence of an external radiation field and/or other mechanisms supporting ionization processes in the medium [10]. This instability can lead to the inhomogeneous distribution of dust particles over the cloud volume and formation of compact clumps where interstellar dust is concentrated. In this case, there is no dust between clumps.

In this work, we analyze the chemical evolution of the diffuse molecular cloud in the model that includes "clumps"—compact cold gas-dust clouds with a radius of $R_c \leq 1$ au, where all interstellar dust grains are concentrated. Estimates of the dust temperature in clumps were taken from [11]. Based on estimates from [10, 12], we assume that the gas temperature in clumps is equal to dust temperature and thus significantly lower than gas temperature in the case of the medium

without clumps. The cold gas in clumps is in hydrostatic equilibrium with surrounding hotter environment and thus denser than in the case of the medium without clumps. This affects the chemical processes on dust particles surface as the rate of atoms and molecules accretion on dust surface in clumps is higher than in the case of homogeneous gas and dust spatial distribution. It is therefore interesting to investigate whether the presence of clumps in the diffuse cloud significantly affects the chemical evolution of the cloud and allows to mitigate the difference between the model and observed molecular abundances in the diffuse clouds.

This paper is organized as follows. Section 2 is dedicated to a brief description of the compact gas and dust clumps formation mechanism. This section also contains the details of the chemical model, including the method to account for the presence of clumps in the medium. Section 3 describes the results of our model calculations. Finally, in Section 4, we discuss the obtained results, compare it with the observational data, and formulate conclusions of the study.

## 2. THE MODEL DESCRIPTION

### *2.1. "Clumpy" Model of the Diffuse Molecular Cloud*

In work [10] it is shown that gas-dust medium is unstable in the presence of ionization mechanisms (for example, ultraviolet (UV) radiation fields, cosmic rays) and can form compact dusty clouds ("clumps") with sizes varying from fractions to tens of astronomical units. In this subsection, we briefly discuss the main points of the theory of the compact clumps formation of and its effects that are important for the chemical evolution of the medium.

According to [10], the formation of clumps can be explained by the instability in a plasma mixed with dust particles [13–15]. This instability is caused by the attractive shadowing force that is a result of collective interactions between dust particles in a gaseous medium. Both ionized and neutral gas components can contribute to the shadowing forces. Ions recombining with electrons on the dust particles surface always lead to occurrence of attraction between dust particles, while the direction of the force between dust particles caused by interaction with neutral atoms and molecules depends on the difference between dust and gas temperatures. If the gas temperature, $T_{\rm gas}$, is higher than the dust temperature, $T_{\rm dust}$, then dust particles will attract to each other due to interaction with neutral gas, or will push away if $T_{\rm gas} < T_{\rm dust}$ [16]. In the diffuse cloud regions where the gas temperature $T_{\rm gas}$ exceeds 100 K while the dust temperature $T_{\rm dust}$ does not exceed 20 K, the neutral shadowing causes attraction between dust particles [12].

A dust particle in the low-temperature plasma with mild UV radiation acquires a negative charge. The balance between ion and electron flows on the dust particle surface determines its stationary charge. This charge becomes positive in the presence of a significant UV field. The mechanism leading to the formation of instability in the medium acts in a similar way for both the negative and positive dust particles charge.

The shadowing forces compress dust into the compact clumps, where an equilibrium is achieved via mutual electrostatic repulsion between charged dust particles. The dust density inside a clump can be many orders of magnitude higher than the average dust density in the case of homogeneous distribution of dust particles. For example, the maximum value of ratio of the dust density inside the clump to the dust density in the homogeneous case reaches $\sim 10^7$ assuming the size of dust grain particle ~0.03 μm. Dust particles do not stick together inside clumps despite such a high local density due to the strong electrostatic repulsion between equally charged dust particles.

The gas temperature in clumps becomes equal to the temperature of dust since the dust density in clumps is high. This can be explained by the fact that the gas inside clumps is cooled due to frequent collisions with dust, which in turn is cooled by its own thermal radiation [10]. The gas in clumps is in pressure equilibrium with hotter environment around the clumps and thus the gas density gas within the clumps is higher than the one between clumps.

According to [10], for the typical properties of the diffuse cloud (gas density ~100 $\mathrm{cm}^{-3}$, gas temperature ~100 K, visual extinction $\sim 1^m$), clump sizes do not exceed 1 au. Average dust density in such clumps is 6–7 orders of magnitude higher than the average dust density in the environment before the formation of clumps [12]. Average distance between such clumps, $L_{\rm cl}$, is $\sim\sqrt[3]{n_{\rm d}^{\rm cl}/n_{\rm d}^{0}}$ times larger than their characteristic size $R_{\rm c}$, which in turn is inversely proportional to the local gas density. Here, $n_{\rm d}^{\rm cl}$ is the number density of dust inside a clump, and $n_{\rm d}^{0}$ is the average number density of dust particles in the homogeneous medium (this refers to the case when there are no clumps in the diffuse cloud). In the clumpy model, local gas density inside the clumps increases by $T_{\rm gas}/T_{\rm dust}$ times with respect to the gas density outside the clumps, where $T_{\rm gas}$ is the gas temperature outside the clumps, $T_{\rm dust}$ is the dust temperature in the clumps. The total gas volume within clumps is $\approx 10^{-6}$ of the gas volume in the entire diffuse cloud, and the distance between clumps is approximately $10^2$ times larger than their size. There is almost no dust between clumps and the gas density between clumps almost does not change (does not depend) due to formation of clumps, i.e., it is equal to the gas density in the case of the homogeneous dust

and gas distribution in the diffuse cloud ("homogeneous" case, see detailed discussion in [12]).

### *2.2. Modification of the Standard Astrochemical Model for Calculations of the Chemical Evolution of the Diffuse Cloud with Clumps*

In the diffuse cloud with homogeneous dust and gas spatial distribution, the gas temperature is higher than dust temperature [3]. The gas and dust temperatures inside clumps become equal due to high density of dust particles and the efficient exchange of energy between gas and dust. This affects the chemical processes on surfaces of dust particles: the rate of accretion of atoms and molecules on the dust surface inside clumps is $\sqrt{T_g/T_d}$ times higher than in the case of the diffuse cloud without clumps. Since all dust grains are concentrated inside clumps and the gas in clumps is cold, chemical processes on the dust surface occur under conditions which are characteristic for clumps, i.e. at a higher density and lower temperature of the gas around dust grains, even though there is the hot gas in the medium between clumps. The calculations of the chemical evolution of the diffuse cloud with clumps can be carried out using the standard astrochemical model (for example, the MONACO model [17] or similar models) with slight modifications assuming that the characteristic time of gas mixing between clumps and interclump medium is shorter than the characteristic time of atomic and molecular abundance changes due to chemical reactions in the gas phase between clumps. One of the modifications is that the rate of accretion of atoms and molecules on the dust grains surface in the model with clumps should be increased by a factor of $\sqrt{T_g/T_d}$ in comparison to the standard model that describes the diffuse cloud homogeneous dust and gas distribution. The other modification is that the gas temperature must be equal to the dust temperature in clumps during the calculations. The next section provides a detailed description of the used model parameters.

### *2.3. Methods for Calculations of the Chemical Composition*

We used the MONACO computational code [17], which implements the rate equations method and can be used to calculate the chemical composition in the gas phase and on the dust surface under the non-stationary conditions. This code calculates changes in relative abundance for each atom or molecule over selected period of time. The chemical kinetics database from [17] is used that includes 638 molecules and 6002 reactions 216 of which are reactions on the dust surface.

The interactions between gas and dust treated by the model include the accretion of neutral species on the dust surface, thermal desorption and photodesorption of species from the dust surface and dissociative ion recombination on a charged dust particle. The dust particle in the model is a homogeneous sphere with a size of 0.1 μm consisting of amorphous silicate; dust-to-gas mass ratio in the model is of 1%. The probability of adsorption of species on the dust surface is assumed to be 100%, efficiency of the reactive (chemical) desorption is of 1%. Desorption energies of atoms and molecules (except for atomic oxygen) from the dust surface were taken from [18]. The desorption energy of atomic oxygen was taken from [19].

**Table 1.** Initial chemical composition for the models of the diffuse cloud. Abundances are calculated relative to the total number of hydrogen nuclei (H) per unit volume [20]

| Atom | Abundance relative to $n_H$ |
|---|---|
| H | 1.0 |
| He | $8.5 \times 10^{-2}$ |
| N | $6.8 \times 10^{-5}$ |
| O | $4.9 \times 10^{-4}$ |
| C+ | $2.7 \times 10^{-4}$ |
| S+ | $1.3 \times 10^{-5}$ |
| Si+ | $3.2 \times 10^{-5}$ |
| Fe+ | $3.2 \times 10^{-5}$ |
| Na+ | $1.7 \times 10^{-6}$ |
| Mg+ | $3.9 \times 10^{-5}$ |
| Cl+ | $3.2 \times 10^{-7}$ |
| P+ | $2.6 \times 10^{-7}$ |
| F+ | $3.6 \times 10^{-8}$ |

The initial chemical composition presented in Table 1 was taken from [20]. Abundances of species are given relative to the total number of hydrogen nuclei per unit volume. The medium is taken to be electrically neutral.

### *2.4. Physical Parameters of the Models*

The main parameters of our models are the number density of hydrogen atoms, which characterizes the density of the gas phase of the considered medium, dust and gas temperatures, optical extinction characterizing the absorption of interstellar radiation, cosmic rays ionization rate and intensity of the diffuse UV radiation field. The physical parameters used in this study to model the diffuse cloud with homogeneous dust and gas spatial distribution are presented in Table 2. The chosen gas and dust temperatures as well as the gas density correspond to the typical estimates for the diffuse clouds and are taken from [3, 21], cosmic rays ionization rate is taken from [22].

To model the chemical evolution of the diffuse cloud with clumps we used the estimates of the dust temperature and visual extinction for both the cloud and clumps within the cloud from [11]. In accordance

**Table 2.** Physical properties used in the model of diffuse cloud with homogeneous dust and gas spatial distribution. $n$—gas number density in the diffuse cloud; $T_g$—gas temperature; $T_d$—dust temperature; $A_V$—visual extinction of the cloud; $\xi$—ionization rate; $\chi_{UV}$—intensity of UV radiation field in Drain units

| Object | $n$, $cm^{-3}$ | $T_g$, K | $T_d$, K | $A_V$, mag | $\xi$, $s^{-1}$ | $\chi_{UV}$ |
|---|---|---|---|---|---|---|
| Homogeneous model | 100 | 100 | 18 | 0.5 | $1.3 \times 10^{-16}$ | 1.0 |

to [11], we considered two types of models with, respectively, clump sizes of 0.1 and 1 au.

The clump model described in [10] assumes that all dust grains, which are uniformly mixed with gas in the homogeneous model of the diffuse cloud, become collected inside clumps in the clumpy model. Thus, the mass and surface area of dust particles are the same in all three diffuse cloud models considered in this study which are the model without clumps, and two models with clumps having sizes of 0.1 and 1.0 au. At the same time, we assume that there is an active mixing of gas between clumps and the interclump medium in the diffuse cloud models with clumps. The visual extinction of the diffuse cloud in the models with clumps depends on the diffuse cloud extinction in the model with homogeneous dust and gas spatial distribution. In the framework of this study, we used the visual extinction of the diffuse cloud with homogeneous dust and gas distribution $A_V = 1^m$. Since the gas volume in the interclump medium is $10^6$ times larger than the gas volume inside clumps, we neglect the gas-phase chemical reactions under physical conditions in clumps. Moreover, as we assume that all dust is concentrated inside clumps, the chemistry on the dust particles surface is calculated for the physical conditions inside clumps. The parameters of models of the diffuse cloud with clumps are given in Table 3. In summary, the chemical evolution in the gas phase of the diffuse cloud with clumps is calculated with temperature, density and extinction of gas outside clumps while the chemical processes on the dust particles surface are calculated for conditions inside clumps. The conditions inside clumps are indicated by upper index "$c$" in Table 3. Also it should be noted that the rates of photoprocesses on the surface of dust particles including photodesorption are calculated for the extinction value that is a sum of $A_V$ and $A_V^c$, where $A_V^c$ is the visual extinction inside clumps.

## 3. RESULTS

### *3.1. Relative Abundances of Molecules*

Currently at least 63 molecules have been detected in the diffuse medium (see [3] and references therein). Figures 1–3 show the results of the chemical evolution modeling for only 58 of them because $PH_3$ and $ArH^+$ molecules are not included in the used chemical model, and the chemistry of chlorine-bearing molecules (HCl, $HCl^+$, and $H_2Cl^+$) in the model is highly incomplete. Selected molecules were divided into 6 groups depending on their composition for a better understanding of figures: CH-compounds (Fig. 1, Group 1), nitrogen-bearing molecules (Fig. 1, Group 2), sulfur-bearing molecules (Fig. 2, Group 3), phosphorus, fluorine and silicon compounds (Fig. 2, Group 4), complex organic molecules and their precursors (Fig. 3, Group 5), and other molecules, including molecular hydrogen $H_2$, CO molecule, water $H_2O$, simple ions and carbon chains without hydrogen (Fig. 3, Group 6).

One can see from figures that the abundances of molecules belonging to different groups behave differently in the models with and without clumps. Group 1 molecules, simple carbon-bearing molecules containing many compounds with carbon chains, show a significant (2–3 orders of magnitude) increase of the maximum abundances in the models with clumps comparing to the model without clumps. Moreover, the maximum abundances of most of these molecules slightly increase with an increase of the clump size from 0.1 to 1.0 au. Formaldehyde $H_2CO$ is the exception, its maximum abundance in the model with large clumps is smaller by one order of magnitude than in the model with small clumps, and approximately equal to the abundance in the model without clumps.

Behavior of the nitrogen-bearing molecules from Group 2 is opposite to the one for molecules of Group 1.

**Table 3.** Physical properties of the models of the diffuse cloud with clumps. $n$—gas number density in the diffuse cloud; $T_g$—gas temperature between clumps; $T_g^c$—gas temperature inside clumps; $T_d^c$—dust temperature; $A_V^c$—visual extinction for a clump calculated from its edge to its center; $A_V$—the average extinction in the center of the diffuse cloud with clumps for the case when the total amount of dust on the line of sight in the homogeneous diffuse cloud model corresponds to visual extinction for an external observer of $A_V = 1.086^m$; $\xi$—ionization rate; $\chi_{UV}$—intensity of UV radiation field in Drain units

| Object | $n$, $cm^{-3}$ | $T_g$, K | $T_g^c$, K | $T_d^c$, K | $A_V^c$, mag | $A_V$, mag | $\xi$, $s^{-1}$ | $\chi_{UV}$ |
|---|---|---|---|---|---|---|---|---|
| Model with clumps $R_c = 0.1$ au | 100 | 100 | 17.4 | 17.4 | 0.1 | 0.24 | $1.30 \times 10^{-16}$ | 1.0 |
| Model with clumps $R_c = 1.0$ au | 100 | 100 | 15.7 | 15.7 | 0.98 | 0.15 | $1.30 \times 10^{-16}$ | 1.0 |

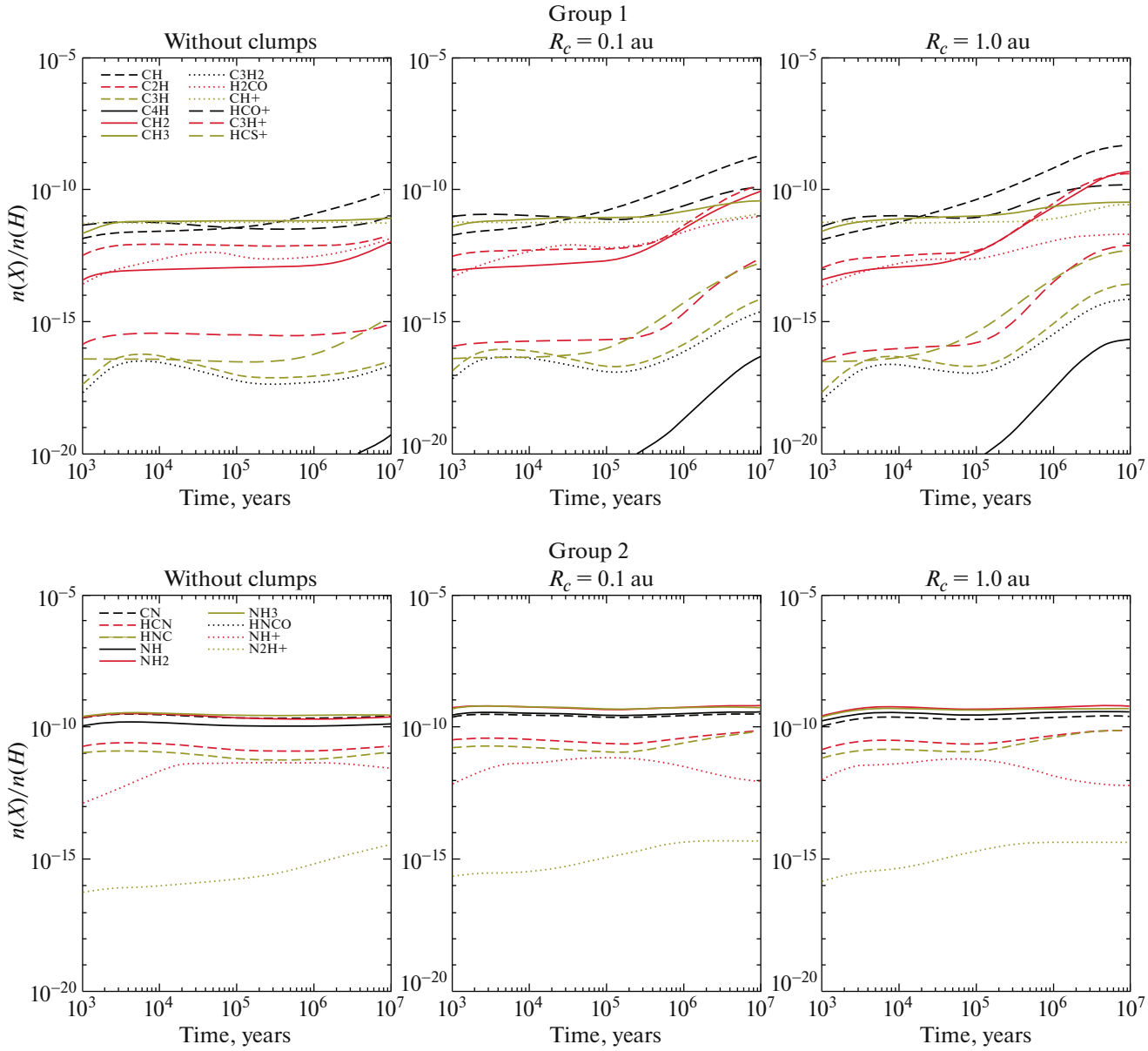


**Fig. 1.** Time dependent change of relative molecular abundances for different models of the diffuse cloud: the model without clumps (on the left panels), with clumps of radius of 0.1 au (on the central panels), with clumps of radius of 1.0 au (on the right panels). Evolution time from $10^3$ to $10^7$ years. Group 1 (upper row) and Group 2 (lower row) of molecules.

Both maximum abundances of these molecules and evolution of abundances with time almost do not differ in all three diffuse cloud models. Even though it is still possible to talk about the increase of molecular abundances in the models with clumps in comparison to the model without clumps, the increase of maximum abundances does not exceed a factor of 2–3. Such changes in abundances can hardly be called significant because they are less than the accuracy of astrochemical modeling [23] as well as the accuracy of the molecular abundance estimates from observations.

Sulfur-bearing molecules from Group 3 behave, in general, similarly to nitrogen-bearing molecules. HS, NS, and CS molecules are the exceptions whose maximum abundances in the models with clumps increase by 1.5–2 orders of magnitude comparing to the model without clumps. The maximum abundances of other molecules from Group 3 vary within an order of magnitude from model to model. It should be noted that the chemistry of sulfur compounds in our chemical model does not include recent improvements proposed in [24]. Therefore, the conclusion about low

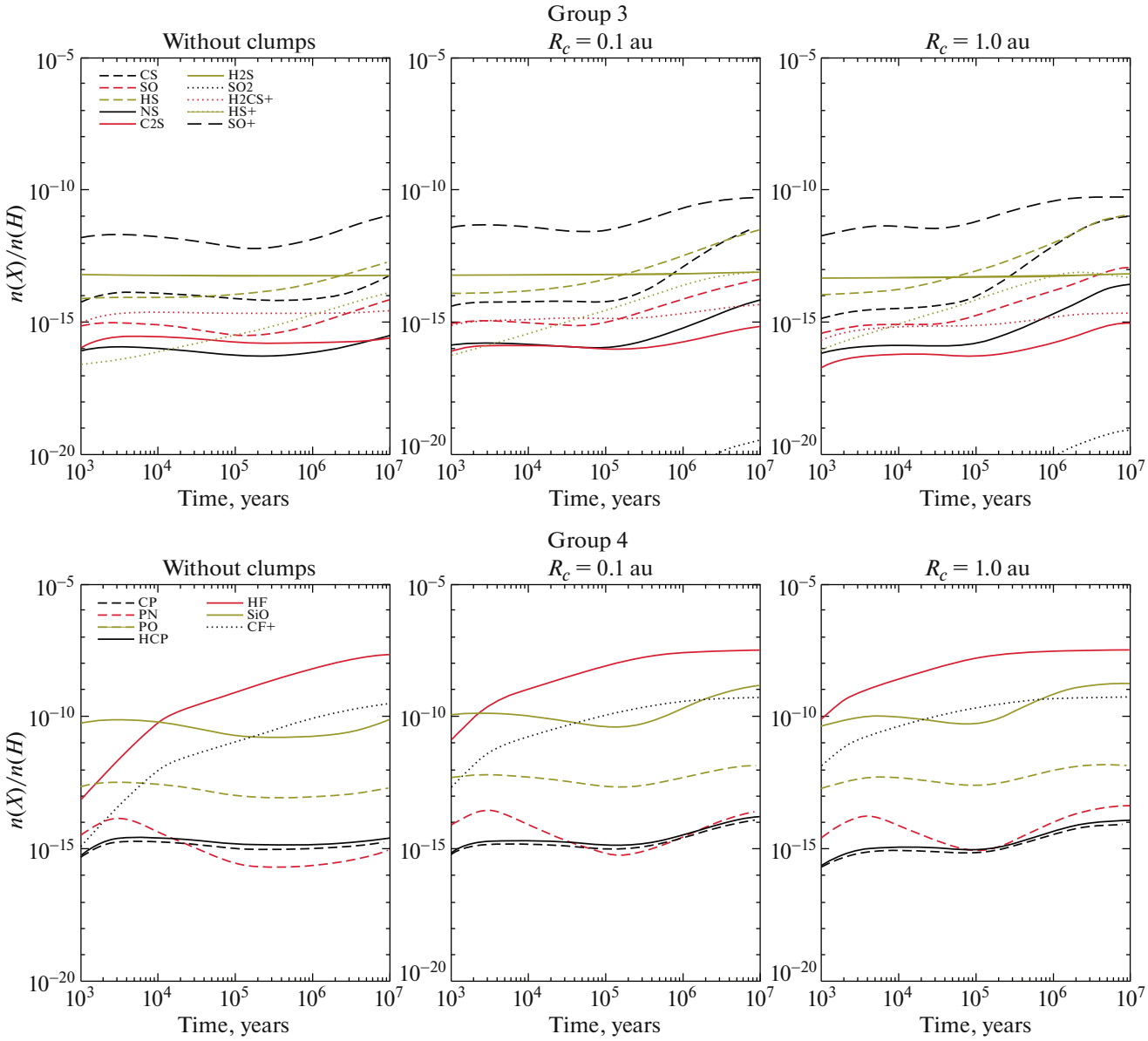


**Fig. 2.** Time dependent change of relative molecular abundances for different models of the diffuse cloud: the model without clumps (on the left panels), with clumps of radius of 0.1 au (on the central panels), with clumps of radius of 1.0 au (on the right panels). Evolution time from $10^3$ to $10^7$ years. Group 3 (upper row) and Group 4 (lower row) of molecules.

impact of clumps presence on sulfur-bearing molecules should be taken with caution.

Group 4 includes phosphorus and fluorine molecular compounds as well as silicon monoxide SiO. The presence clumps also has a negligible effect on the chemical evolution of molecules from this group. One can see in Fig. 2 that maximum abundances of all Group 4 molecules change by less than a factor of 2–3. PO molecule is some kind of exception whose minimum abundance in the models with clumps becomes an order of magnitude higher than in the model without clumps. It is interesting to note that our model abundances of PN, PO, CP, and HCP molecules are lower by 4–5 orders of magnitude than in the "best-fit" model of phosphorus chemistry in the diffuse medium published in [25]. However, in the model of [25], relatively high abundances of phosphorus-bearing molecules are achieved only at visual extinction values $A_V$ equal to or greater than $3.0^m$. The authors of [25] explain the choice of relatively high visual extinction value $A_V$, which is typical for a translucent clouds, assuming that at line of sight there can be regions of denser medium where in reality, apparently, there are phosphorus-bearing molecules with high molecular

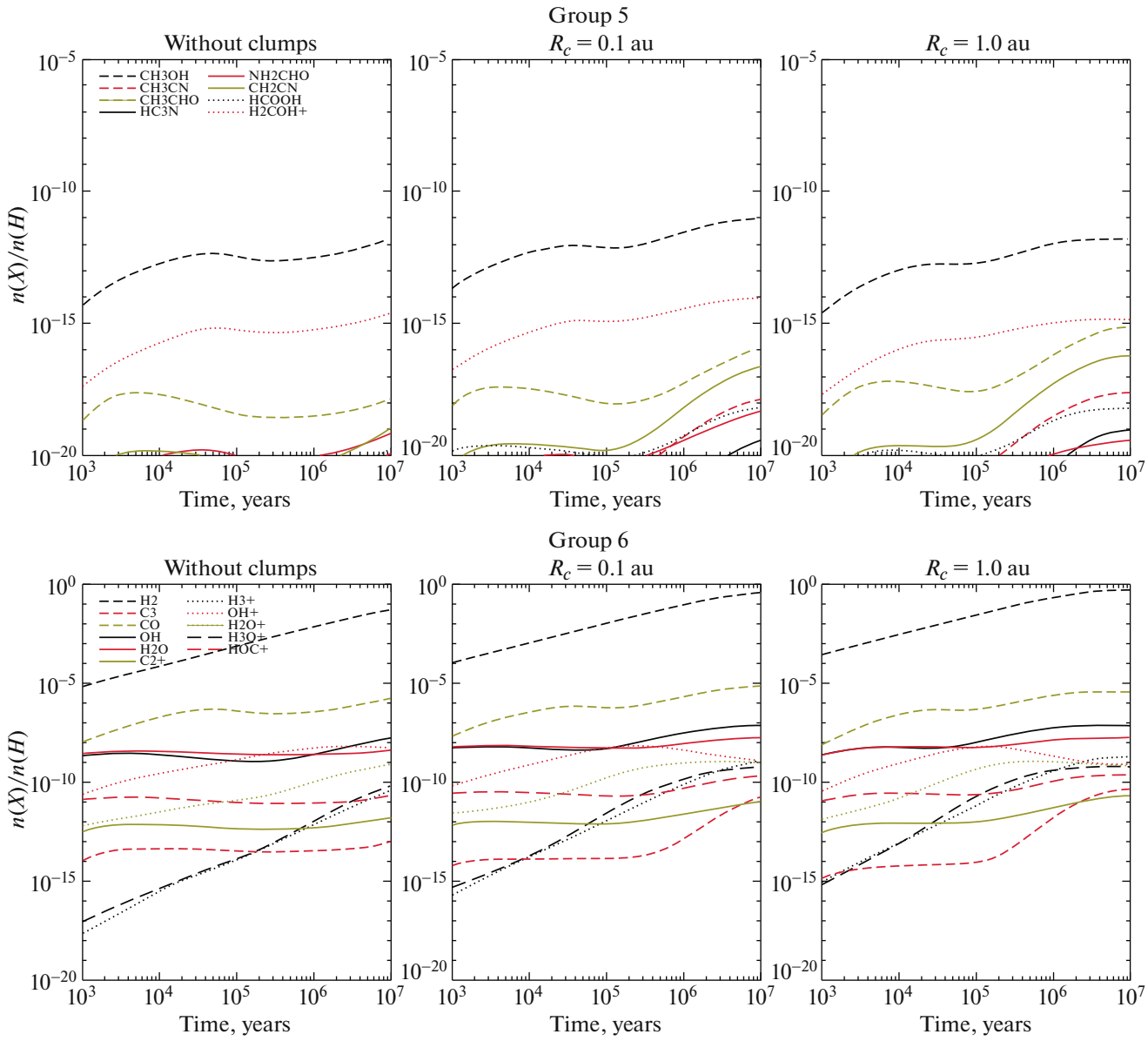


**Fig. 3.** Time dependent change of relative molecular abundances for different models of the diffuse cloud: the model without clumps (on the left panels), with clumps of radius of 0.1 au (on the central panels), with clumps of radius of 1.0 au (on the right panels). Evolution time from $10^3$ to $10^7$ years. Group 5 (upper row) and Group 6 (lower row) of molecules.

abundances with respect to hydrogen. At the same time, the phosphorus-bearing molecule abundances obtained in [25] for $A_V = 1^m$ (authors do not consider smaller values) approach the model values obtained in our work.

Group 5 includes complex organic molecules and their precursors—compounds whose detection in the diffuse medium perhaps was the most unexpected. The presence or absence of clumps in the diffuse cloud does not affect significantly the chemical evolution of complex molecules as for molecules from the previous group. It is seen in Fig. 3, that both the models of diffuse cloud with and without clumps considered in this study do not explain the observed abundances of complex molecules with the exception for methanol $CH_3OH$, which model abundance is close to the observed one. Apparently, the failure of diffuse cloud models to reproduce the observed abundances of complex organic molecules indicates that these molecules form in a denser gas of translucent clouds that can present on a line of sight in observations of diffuse clouds. Methanol is the exception to this rule because its formation on the dust particles surface is effective even at dust temperatures characteristic for diffuse molecular clouds.

Finally, Group 6 includes molecules which are chemically dissimilar. As the consequence of this dissimilarity, their evolution in models with and without clumps proceeds differently.

One should note the difference in rates of atomic to molecular hydrogen conversion in all three models of the diffuse cloud. As it is seen in Fig. 3, the time of atomic to molecular hydrogen transition in the models with clumps is higher by more than an order of magnitude in comparison to the model without clumps. This fact is important for the chemical evolution of other molecules as the presence of molecular hydrogen is necessary for the occurrence of effective ion-molecular chemistry in gas phase. Moreover, the $H \rightarrow H_2$ transition time indicates in favor of the scenario of giant molecular clouds formation in large-scale turbulent flows (see more discussion in [12]).

The presence or absence of clumps does not significantly affect the other molecules from Group 6, the changes of their abundance does not exceed an order of magnitude. $C_3$ molecule is the exception to this as its maximum abundance in the models with clumps increases by 3 orders of magnitude comparing with the model without clumps. $C_3$ is found in many observations of a diffuse medium. Apparently, it is not surprising as the relatively high abundance of this molecule was achieved even in our model of the diffuse cloud without clumps characterized by a low gas density and low visual extinction. The presence of clumps is the necessary condition for $C_3$ to achieve the high abundance relative to hydrogen in the diffuse cloud.

Table 4 shows maximum model abundances of molecules that have been detected in the diffuse clouds. Right column of Table 4 shows molecular abundances obtained from observations of diffuse clouds. In such observations, the same line-of-sight may cross many regions that are not evolutionary related to each other. In this situation, it seems pointless for us to determine the "time of the best agreement" between the model and observations as it is often done during modeling of individual objects in star formation regions. For this reason, we perform comparison of the observational data with the maximum model abundances despite that they are reached at different points in time instead of comparison of observations with the molecular abundances set calculated for one "best-fit" point in time.

One can see from Table 4, that the model without clumps reproduces abundances of 10 molecules within an order of magnitude, and both the models with clumps reproduce abundances of 12 out of 28 molecules for which we were able to summarize the observational data. Agreement between models and observational data is far from the complete one and the presence of clumps in the model only slightly improves it. The maximum abundances of most molecules in our model with low gas density and visual extinction are several orders of magnitude lower than values obtained from observations.

### *3.2. Ratios of Molecular Abundances*

Ratios of molecular abundances are often determined from observations more accurately than the relative molecular abundances. Therefore, for better understanding of how clumps affect the diffuse cloud chemical evolution, we also analyzed the effect of clumps on the abundance ratios. The abundance ratios calculated in all three diffuse cloud models considered in this study are given in Tables 5–7 along with observed estimates of ratios obtained for sightlines toward different sources from literature. The studies from which the observed abundance ratios were taken are given in the last column of Tables 5–7. The dependence of our calculated abundance ratios on time is shown in Figs. 4–6. All ratios are randomly divided into 5 groups.

In all three considered diffuse cloud models, there are abundance ratios whose values differ significantly from the observed values. For example, the differences can reach 10 orders of magnitude for $C_4H/C_2H$, $HC_3N/HCN$, and $SO_2/HCO^+$ ratios. This can be related to the fact that the conditions in a given observed object can differ from the typical ones used in our calculations and derived based on observations of many objects.

Our results show that the models with clumps match the observations better than the model without clumps. The agreement between the models and observations becomes better with increasing clump radius. As seen from Tables 5–7, the models without clumps predict 16 abundance ratios that are consistent with the observational data. In the models with clumps of various radii, there were 20 ratios that match the observations: 16 of them are the same as in the model without clumps and 4 additional ratios are $C_2H/HCO^+$, $HCN/C_2H$, CS/HCN, and OH/CH (see Tables 6 and 7).

The model $C_2H_3N/HC_3N$, $CS/HCS^+$, $CS/C_2H$, $SO/H_2S$, $H_2O^+/H_3O^+$, $OH^+/H_2O^+$, and $HS/H_2S$ ratios become better consistent to observations with increasing clump radius. The minimum difference between the model and observed values of all these ratios except $HS/H_2S$ is achieved $10^5$–$10^6$ years of the diffuse cloud chemical evolution. The model $HS/H_2S$ ratio matches the observations best in the time range of $10^6$–$10^8$ years (see Table 7).

It should be noted that for some ratios the agreement between the model and observed values is a bit worse in the models with clumps than in the model without clumps. The model $HS/H_2S$ ratio corresponds to the observed one equally good at all considered timescales of the chemical evolution of the diffuse cloud without clumps (the observed ratio and the ratio

**Table 4.** The molecular abundances in the diffuse cloud models without clumps and with clumps with $R_c$ = 0.1 and 1.0 au in comparison to the observed abundances in the diffuse clouds. The molecules in bold are those with the model abundances that are close to the observed ones. Only molecules with observed relative abundance estimates existing in the literature are presented. Observational data is taken from [4–7, 25, 27–34]

| Molecule | Model without clumps | Model with clumps $R_c$ = 0.1 au | Model with clumps $R_c$ = 1.0 au | Observations |
|---|---|---|---|---|
| C2H | 1.60E–11 | 2.15E–10 | 4.00E–10 | 2.90E–08 |
| C3H | 2.97E–16 | 1.17E–14 | 2.53E–14 | 2.00E–10 |
| C3H2 | 1.55E–16 | 3.92E–15 | 7.36E–15 | 1.40E–09 |
| C3 | 1.20E–12 | 2.441E–11 | 4.380E–11 | 1.10E–09 |
| CN | 3.43E–10 | 3.36E–10 | 2.72E–10 | 1.50E–08 |
| HCN | 2.97E–11 | 7.83E–11 | 7.66E–11 | 0.30E–08 |
| **HNC** | 2.16E–11 | **7.47E–11** | **7.60E–11** | 7.00E–10 |
| CS | 5.16E–13 | 5.64E–12 | 9.92E–12 | 1.42E–09 |
| SO | 1.91E–14 | 5.43E–14 | 1.15E–13 | 4.52E–10 |
| H2S | 6.07E–14 | 7.86E–14 | 6.45E–14 | 2.44E–09 |
| **CH** | 3.23E–10 | **2.50E–09** | **4.80E–09** | 1.96E–08 |
| CH+ | 5.93E–12 | 1.43E–11 | 2.79E–11 | 4.18E–09 |
| **NH3** | **3.54E–10** | **5.98E–10** | **5.19E–10** | 3.00E–09 |
| H2CO | 6.40E–12 | 1.00E–11 | 2.05E–12 | 0.40E–08 |
| **NH** | **1.60E–10** | **3.92E–10** | **4.01E–10** | 4.95E–09 |
| **OH** | **3.99E–08** | **7.00E–08** | **6.77E–08** | 1.00E–07 |
| **CO** | **7.16E–06** | **6.90E–06** | **3.45E–06** | 5.35E–06 |
| HCO+ | 3.66E–11 | 1.36E–10 | 1.50E–10 | 0.30E–08 |
| CH3CN | **1.32E–19** | **1.83E–18** | **2.44E–18** | <0.40E–10 |
| CH3OH | 6.85E–12 | 9.27E–12 | 1.50E–12 | 8.10E–08* |
| N2H+ | **5.16E–15** | **5.22E–15** | **4.57E–15** | <0.40E–11 |
| HS | 5.98E–13 | 4.33E–12 | 1.16E–11 | 4.96E–09 |
| HS+ | 3.56E–14 | 7.64E–14 | 7.57E–14 | 1.16E–09 |
| CH2 | 7.26E–12 | 1.32E–10 | 4.96E–10 | 1.60E–08 |
| **NH2** | **3.35E–10** | **6.53E–10** | **6.48E–10** | 4.00E–09 |
| **H2O** | **8.65E–09** | **1.74E–08** | **1.65E–08** | 2.40E–08 |
| **H3O+** | **2.36E–10** | **5.60E–10** | **5.78E–10** | 2.50E–09 |
| **HF** | **2.89E–08** | **3.27E–08** | **3.31E–08** | 1.40E–08 |
| PN | 1.45E–14 | 3.42E–14 | 4.40E–14 | <4.90E–11 |
| PO | 5.86E–13 | 1.51E–12 | 1.47E–12 | <5.00E–10 |
| CP | 5.71E–15 | 1.37E–14 | 8.30E–15 | <2.60E–09 |

*According to [26], the obtained values of the methanol relative abundance are overestimated due to a possibly underestimated value of column density of molecular hydrogen.

in the model without clumps are 1.25 and 3.20, respectively, see Table 5). The models with clumps with $R_c$ = 0.1 and 1.0 au explain the observed $HS/H_2S$ ratio only at time points of $10^5$ and $10^6$ years (see Tables 6 and 7). $CS/H_2S$ and CS/SO ratios in the model without clumps are in good agreement with the observed ones (6.0 and 1.7, respectively) at timescale of $10^6$–$10^8$ years, while, in the model with $10^7$ au, the agreement is achieved only at $10^6$ and $10^5$ years, respectively (see Table 7). This discrepancy with observations can be related to incompleteness of the data for chemistry of sulfur-bearing compounds [24].

**Table 5.** The abundance ratio values in the model of the diffuse cloud without clumps for different moments in time in comparison with the observed ratios in the diffuse clouds. The ratios in bold are those with values which are close to the observed ones

| Ratio | $10^5$ years | $10^6$ years | $10^7$ years | $10^8$ years | Observation | Source |
|---|---|---|---|---|---|---|
| C2H/HCO+ | 2.26E–001 | 2.36E–001 | 2.09E–001 | 4.39E–001 | 1.45E+001 | [4] |
| C2H/C3H | 7.70E+004 | 8.77E+004 | 5.61E+004 | 5.40E+004 | 2.00E+002 | [35] |
| C3H2/HCO+ | 1.75E–006 | 1.59E–006 | 2.29E–006 | 4.24E–006 | 7.00E–001 | [4] |
| C4H/C2H | 3.21E–009 | 4.20E–009 | 2.49E–008 | 7.14E–008 | 1.00E+000 | [35] |
| **CN/HCN** | **1.71E+001** | **1.74E+001** | **1.35E+001** | **1.02E+001** | 6.80E+000 | [5] |
| HCN/C2H | 1.80E+001 | 1.69E+001 | 9.83E+000 | 1.86E+000 | 8.00E–002 | [5] |
| **HCN/HCO+** | **4.05E+000** | **3.99E+000** | **2.05E+000** | **8.14E–001** | 1.97E+000 | [5] |
| **HCN/HNC** | **2.11E+000** | **2.06E+000** | **1.71E+000** | **1.38E+000** | 5.00E+000 | [35] |
| HC3N/HCN | 5.30E–011 | 5.17E–011 | 6.38E–011 | 1.46E–010 | 4.00E–001 | [35] |
| **C2H3N/HC3N** | 1.96E–001 | 3.79E–001 | **9.64E+000** | **3.03E+001** | 4.00E+000 | [35] |
| CS/HCO+ | 2.09E–003 | 2.27E–003 | 5.78E–003 | 1.41E–002 | 2.00E+000 | [6] |
| CS/HCN | 5.16E–004 | 5.69E–004 | 2.81E–003 | 1.73E–002 | 7.00E–001 | [6] |
| **CS/H2S** | 1.32E–001 | 1.39E–001 | **9.52E–001** | **7.91E+000** | 6.00E+000 | [6] |
| **CS/SO** | 2.14E+001 | **9.17E+000** | **8.32E+000** | 2.70E+001 | 1.70E+000 | [6] |
| **CS/HCS+** | 2.37E+002 | **1.28E+002** | **3.53E+001** | **3.55E+001** | 1.33E+001 | [6] |
| **CS/C2H** | 9.27E–003 | 9.62E–003 | **2.77E–002** | **3.22E–002** | 1.30E–001 | [6] |
| SO/HCO+ | 9.78E–005 | 2.48E–004 | 6.94E–004 | 5.24E–004 | 9.00E–001 | [6] |
| **SO/H2S** | 6.19E–003 | 1.52E–002 | **1.14E–001** | **2.93E–001** | 2.40E–001 | [7] |
| SO2/HCO+ | 1.80E–011 | 5.01E–011 | 2.98E–010 | 4.19E–010 | 5.00E–001 | [6] |
| H2S/HCO+ | 1.58E–002 | 1.63E–002 | 6.07E–003 | 1.79E–003 | 2.70E–001 | [6] |
| HCS+/HCO+ | 8.81E–006 | 1.77E–005 | 1.64E–004 | 3.97E–004 | 1.30E–001 | [6] |
| OH/CH | 2.86E+002 | 1.87E+002 | 1.85E+002 | 1.24E+002 | 3.00E+000 | [35] |
| NH3/CS | 3.99E+004 | 3.74E+004 | 5.49E+003 | 6.39E+002 | 1.00E+000 | [28] |
| NH3/H2CO | 9.13E+002 | 9.52E+002 | 2.18E+002 | 5.15E+001 | 4.00E–001 | [28] |
| **H2CO/CS** | 4.38E+001 | 3.93E+001 | 2.52E+001 | **1.24E+001** | 2.30E+000 | [28] |
| **H2O** | 9.13E+002 | 9.89E+001 | **1.22E+001** | **4.35E+000** | 1.50E+000 | [8] |
| **OH+/H2O+** | 1.12E+002 | 4.96E+001 | **7.15E+000** | **2.90E+000** | 4.00E+000 | [8] |
| **OH+/H3O+** | 1.02E+005 | 4.90E+003 | 8.76E+001 | **1.26E+001** | 6.00E+000 | [8] |
| **HS/H2S** | **2.06E–001** | **5.55E–001** | **3.20E+000** | **9.16E+000** | 1.25E+000 | [7] |
| HS+/CH | 5.60E–005 | 3.29E–004 | 2.29E–003 | 6.01E–003 | 2.80E–001 | [9] |
| HOC+/HCO+ | 2.65E+000 | 2.62E+000 | 2.13E+000 | 1.79E+000 | 1.50E–002 | [36] |
| HCO+/HF | 4.15E–003 | 5.00E–004 | 4.34E–004 | 1.26E–003 | 2.50E–001 | [36] |
| **HOC+/HF** | **1.10E–002** | **1.31E–003** | **9.26E–004** | **2.26E–003** | 4.00E–003 | [36] |
| **CF+/HF** | **1.32E–002** | **1.28E–002** | **1.41E–002** | **1.51E–002** | 1.70E–002 | [36] |

In the model of the diffuse cloud without clumps, many abundance ratios reach stationary values quickly. The examples of such ratios are CN/HCN, $C_3H_2/HCO^+$, HNC/HCN, and $CS/HCO^+$ in Fig. 4, $SO/HCO^+$, $HCS^+/HCO^+$, and $SO/H_2S$ in Fig. 5, and $HS^+/CH^+$ in Fig. 6. In the models with clumps, the values of these ratios not only decrease or increase but also show a noticeable change over time in comparison to the model without clumps. Such a behavior of molecular abundance ratios in the models with clumps allows one to implement the chemical clock method more widely and efficiently.

In general, in terms of agreement between the model and observations, the presence of clumps in the diffuse cloud does not affect negatively the chemical evolution of the cloud, and in some cases it even helps to achieve better agreement between the model and observed values.

**Table 6.** The abundance ratio values in the model of the diffuse cloud with clumps with the radius $R_c = 0.1$ au for different moments in time in comparison with the observed ratios in the diffuse clouds. The ratios in bold are those with values which are close to the observed ones

| Ratio | $10^5$ years | $10^6$ years | $10^7$ years | $10^8$ years | Observation | Source |
|---|---|---|---|---|---|---|
| **C2H/HCO+** | 7.67E–002 | 1.74E–001 | 1.19E+000 | **1.58E+000** | 1.45E+001 | [4] |
| C2H/C3H | 2.64E+004 | 3.21E+004 | 2.10E+004 | 1.83E+004 | 2.00E+002 | [35] |
| C3H2/HCO+ | 1.75E–006 | 2.93E–006 | 1.99E–005 | 2.87E–005 | 7.00E–001 | [4] |
| C4H/C2H | 8.00E–009 | 4.61E–008 | 3.31E–007 | 4.35E–007 | 1.00E+000 | [35] |
| **CN/HCN** | **1.02E+001** | **7.43E+000** | **4.58E+000** | **4.37E+000** | 6.80E+000 | [5] |
| **HCN/C2H** | 4.30E+001 | 9.23E+000 | **5.01E–001** | **3.64E–001** | 8.00E–002 | [5] |
| **HCN/HCO+** | **3.30E+000** | **1.61E+000** | **5.96E–001** | **5.75E–001** | 1.97E+000 | [5] |
| **HCN/HNC** | **2.06E+000** | **1.52E+000** | **1.07E+000** | **1.05E+000** | 5.00E+000 | [35] |
| HC3N/HCN | 1.74E–011 | 3.14E–011 | 5.15E–010 | 7.58E–010 | 4.00E–001 | [35] |
| **C2H3N/HC3N** | **1.43E+000** | 4.19E+001 | **3.63E+001** | **3.09E+001** | 4.00E+000 | [35] |
| CS/HCO+ | 7.85E–004 | 4.89E–003 | 3.12E–002 | 4.14E–002 | 2.00E+000 | [6] |
| **CS/HCN** | 2.38E–004 | 3.04E–003 | 5.23E–002 | **7.21E–002** | 7.00E–001 | [6] |
| **CS/H2S** | 9.62E–002 | **1.80E+000** | **5.00E+001** | 7.18E+001 | 6.00E+000 | [6] |
| **CS/SO** | **6.02E+000** | **1.61E+001** | 9.38E+001 | 1.04E+002 | 1.70E+000 | [6] |
| **CS/HCS+** | **5.84E+001** | **2.28E+001** | **2.41E+001** | **2.42E+001** | 1.33E+001 | [6] |
| **CS/C2H** | 1.02E–002 | **2.80E–002** | **2.62E–002** | **2.62E–002** | 1.30E–001 | [6] |
| SO/HCO+ | 1.31E–004 | 3.03E–004 | 3.33E–004 | 3.98E–004 | 9.00E–001 | [6] |
| **SO/H2S** | 1.60E–002 | **1.11E–001** | **5.33E–001** | **6.91E–001** | 2.40E–001 | [7] |
| SO2/HCO+ | 2.16E–011 | 1.28E–010 | 2.84E–010 | 3.49E–010 | 5.00E–001 | [6] |
| H2S/HCO+ | 8.16E–003 | 2.72E–003 | 6.24E–004 | 5.77E–004 | 2.70E–001 | [6] |
| HCS+/HCO+ | 1.34E–005 | 2.14E–004 | 1.29E–003 | 1.71E–003 | 1.30E–001 | [6] |
| **OH/CH** | 2.80E+002 | 1.61E+002 | 3.72E+001 | **2.79E+001** | 3.00E+000 | [35] |
| NH3/CS | 8.91E+004 | 4.73E+003 | 1.54E+002 | 1.05E+002 | 1.00E+000 | [28] |
| NH3/H2CO | 8.24E+002 | 2.32E+002 | 6.38E+001 | 5.91E+001 | 4.00E–001 | [28] |
| **H2CO/CS** | 1.08E+002 | **2.04E+001** | **2.41E+000** | **1.77E+000** | 2.30E+000 | [28] |
| **H2O** | 6.38E+001 | **6.74E+000** | **1.53E+000** | **1.35E+000** | 1.50E+000 | [8] |
| **OH+/H2O+** | **3.15E+001** | **4.17E+000** | **1.38E+000** | **1.28E+000** | 4.00E+000 | [8] |
| **OH+/H3O+** | 2.01E+003 | **2.81E+001** | **2.11E+000** | **1.72E+000** | 6.00E+000 | [8] |
| **HS/H2S** | **6.88E–001** | **4.83E+000** | 3.91E+001 | 5.51E+001 | 1.25E+000 | [7] |
| HS+/CH | 4.72E–004 | 3.81E–003 | 6.62E–003 | 5.33E–003 | 2.80E–001 | [9] |
| HOC+/HCO+ | 2.61E+000 | 2.02E+000 | 1.56E+000 | 1.54E+000 | 1.50E–002 | [36] |
| HCO+/HF | 8.86E–004 | 9.25E–004 | 3.80E–003 | 4.17E–003 | 2.50E–001 | [36] |
| **HOC+/HF** | **2.31E–003** | **1.87E–003** | **5.94E–003** | **6.40E–003** | 4.00E–003 | [36] |
| **CF+/HF** | **1.34E–002** | **1.47E–002** | **1.61E–002** | **1.62E–002** | 1.70E–002 | [36] |

## 4. DISCUSSION AND CONCLUSIONS

In this work, we consider the model of diffuse molecular cloud characterized by low gas density ($n_H = 100$ cm$^{-3}$) and visual extinction, which is very important for the cloud chemical evolution. The typical line-of-sight visual extinction for the diffuse cloud is of $A_V = 1^m$, but in our chemical model we consider the halved value of $A_V = 0.5^m$ because it is assumed that the diffuse cloud is illuminated by UV radiation from all sides. Under the chosen physical conditions the chemical model without clumps expectedly predicts the abundance values for many molecules that are lower by many orders of magnitude than those estimated from observations. The main goal of this work was to study whether the presence of compact gas-dust clumps in the diffuse cloud, which existence is predicted in [10], can lead to the significant increase of

**Table 7.** The abundance ratio values in the model of the diffuse cloud with clumps with the radius $R_c$ = 1.0 au for different moments in time in comparison with the observed ratios in the diffuse clouds. The ratios in bold are those with values which are close to the observed ones

| Ratio | $10^5$ years | $10^6$ years | $10^7$ years | $10^8$ years | Observation | Source |
|---|---|---|---|---|---|---|
| **C2H/HCO+** | 5.62E–002 | 4.28E–001 | **2.63E+000** | **2.67E+000** | 1.45E+001 | [4] |
| C2H/C3H | 2.51E+004 | 3.75E+004 | 1.59E+004 | 1.58E+004 | 2.00E+002 | [35] |
| C3H2/HCO+ | 1.26E–006 | 4.64E–006 | 4.81E–005 | 4.91E–005 | 7.00E–001 | [4] |
| C4H/C2H | 1.43E–008 | 8.66E–008 | 5.29E–007 | 5.34E–007 | 1.00E+000 | [35] |
| **CN/HCN** | **8.30E+000** | **4.91E+000** | **3.55E+000** | **3.55E+000** | 6.80E+000 | [5] |
| **HCN/C2H** | 4.81E+001 | 1.70E+000 | **1.94E–001** | **1.91E–001** | 8.00E–002 | [5] |
| **HCN/HCO+** | **2.70E+000** | **7.27E–001** | **5.11E–001** | **5.11E–001** | 1.97E+000 | [5] |
| **HCN/HNC** | **1.95E+000** | **1.21E+000** | **1.01E+000** | **1.01E+000** | 5.00E+000 | [35] |
| HC3N/HCN | 8.11E–012 | 8.63E–011 | 1.20E–009 | 1.22E–009 | 4.00E–001 | [35] |
| **C2H3N/HC3N** | **1.29E+001** | 7.14E+001 | **2.63E+001** | **2.61E+001** | 4.00E+000 | [35] |
| CS/HCO+ | 1.03E–003 | 1.10E–002 | 6.51E–002 | 6.62E–002 | 2.00E+000 | [6] |
| **CS/HCN** | 3.81E–004 | 1.52E–002 | **1.28E–001** | **1.30E–001** | 7.00E–001 | [6] |
| **CS/H2S** | 1.89E–001 | **1.35E+001** | 1.51E+002 | 1.54E+002 | 6.00E+000 | [6] |
| **CS/SO** | **5.07E+000** | 4.82E+001 | 8.71E+001 | 8.63E+001 | 1.70E+000 | [6] |
| **CS/HCS+** | **2.31E+001** | **1.98E+001** | **2.05E+001** | **2.05E+001** | 1.33E+001 | [6] |
| **CS/C2H** | **1.83E–002** | **2.58E–002** | **2.48E–002** | **2.48E–002** | 1.30E–001 | [6] |
| SO/HCO+ | 2.03E–004 | 2.29E–004 | 7.48E–004 | 7.67E–004 | 9.00E–001 | [6] |
| **SO/H2S** | **3.72E–002** | **2.79E–001** | **1.73E+000** | **1.78E+000** | 2.40E–001 | [7] |
| SO2/HCO+ | 3.90E–011 | 1.35E–010 | 5.54E–010 | 5.68E–010 | 5.00E–001 | [6] |
| H2S/HCO+ | 5.45E–003 | 8.19E–004 | 4.31E–004 | 4.31E–004 | 2.70E–001 | [6] |
| HCS+/HCO+ | 4.45E–005 | 5.56E–004 | 3.18E–003 | 3.23E–003 | 1.30E–001 | [6] |
| **OH/CH** | 2.39E+002 | 8.19E+001 | **1.43E+001** | **1.41E+001** | 3.00E+000 | [35] |
| NH3/CS | 5.12E+004 | 6.81E+002 | 5.33E+001 | 5.23E+001 | 1.00E+000 | [28] |
| NH3/H2CO | 2.03E+003 | 4.48E+002 | 2.54E+002 | 2.53E+002 | 4.00E–001 | [28] |
| **H2CO/CS** | 2.52E+001 | **1.52E+000** | 2.10E–001 | 2.07E–001 | 2.30E+000 | [28] |
| **H2O** | 2.37E+001 | **2.66E+000** | **1.09E+000** | **1.09E+000** | 1.50E+000 | [8] |
| **OH+/H2O+** | **1.30E+001** | **1.98E+000** | **1.14E+000** | **1.14E+000** | 4.00E+000 | [8] |
| **OH+/H3O+** | 3.08E+002 | **5.27E+000** | **1.25E+000** | **1.24E+000** | 6.00E+000 | [8] |
| **HS/H2S** | **1.77E+000** | 1.77E+001 | 1.75E+002 | 1.80E+002 | 1.25E+000 | [7] |
| HS+/CH | 1.17E–003 | 6.92E–003 | 1.78E–003 | 1.72E–003 | 2.80E–001 | [9] |
| HOC+/HCO+ | 2.47E+000 | 1.69E+000 | 1.49E+000 | 1.49E+000 | 1.50E–002 | [36] |
| HCO+/HF | 5.69E–004 | 2.21E–003 | 4.53E–003 | 4.53E–003 | 2.50E–001 | [36] |
| **HOC+/HF** | **1.41E–003** | **3.75E–003** | **6.74E–003** | **6.75E–003** | 4.00E–003 | [36] |
| **CF+/HF** | **1.37E–002** | **1.57E–002** | **1.64E–002** | **1.64E–002** | 1.70E–002 | [36] |

the maximum abundances of molecules whose observed abundances are not explained by the model without clumps. The results described in previous section give a negative answer to this question in general. Indeed, compact gas-dust clouds ("clumps") affect the abundances of a number of molecules and molecular ions observed in the diffuse interstellar clouds, and the maximum abundances of a number of molecules in the models with clumps increase by 2–3 orders of magnitude in comparison to the model without clumps. However, one can see from Table 4 that even maximum abundances of molecules that have increased by several orders of magnitude due to the clumps presence are still lower than the observed ones by several orders of magnitude. Moreover, there is a significant number of molecules whose abundances

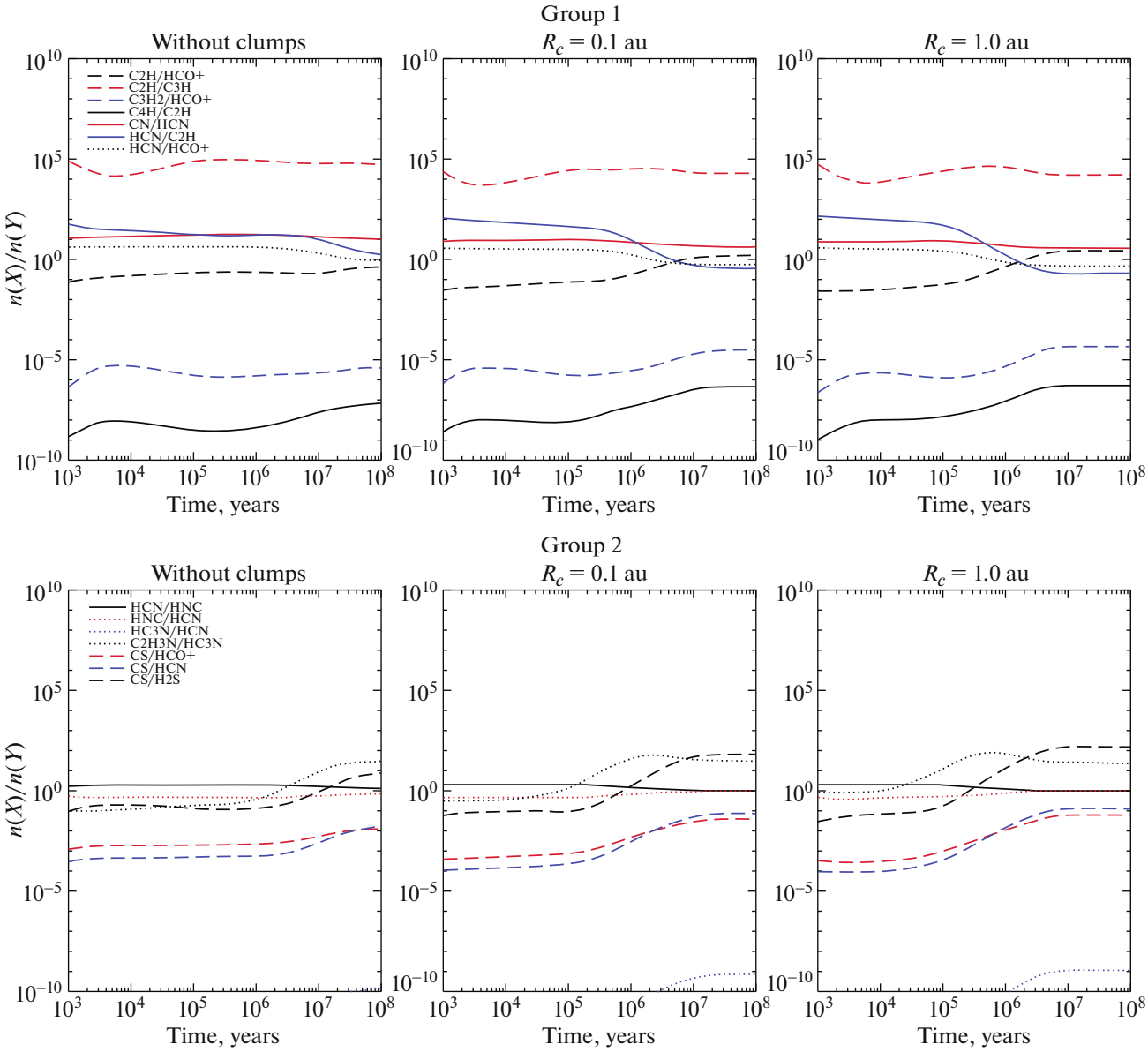


**Fig. 4.** Time dependent change of ratios of molecular abundances for different models of the diffuse cloud: the model without clumps (on the left panels), with clumps of radius of 0.1 au (on the central panels), with clumps of radius of 1.0 au (on the right panels). Evolution time from $10^3$ to $10^8$ years. Group 1 (upper row) and Group 2 (lower row) of molecules.

behave in almost exactly the same way in all considered models with and without clumps. Nonetheless, there are two molecules whose abundances in the models with clumps are close to the observed values: HNC and CH. Also, the abundance of $C_3$ molecule, which have been found in many studies of the diffuse medium (that indicates its prevalence), is almost satisfy the criterion of agreement with observations in the models with clumps. Below we consider the features of the chemical evolution of some representative molecules that can be an example of how the presence of clumps affects the evolution of the diffuse cloud molecular composition.

Group 1 of molecules described in previous section (upper row in Fig. 1) includes simple carbon-bearing molecules that form in the gas phase in ion-molecule chemical reactions. Abundances of these molecules increase during the late times of the cloud chemical evolution in the models with clumps because these abundances depend directly on the amount of molecular hydrogen ($H_2$) in the gas phase. As the $H \rightarrow H_2$ transition is faster by approximately an order of magnitude in the models with clumps comparing to the model without clumps, the hydrogen at late times of the cloud evolution is predominantly in molecular and

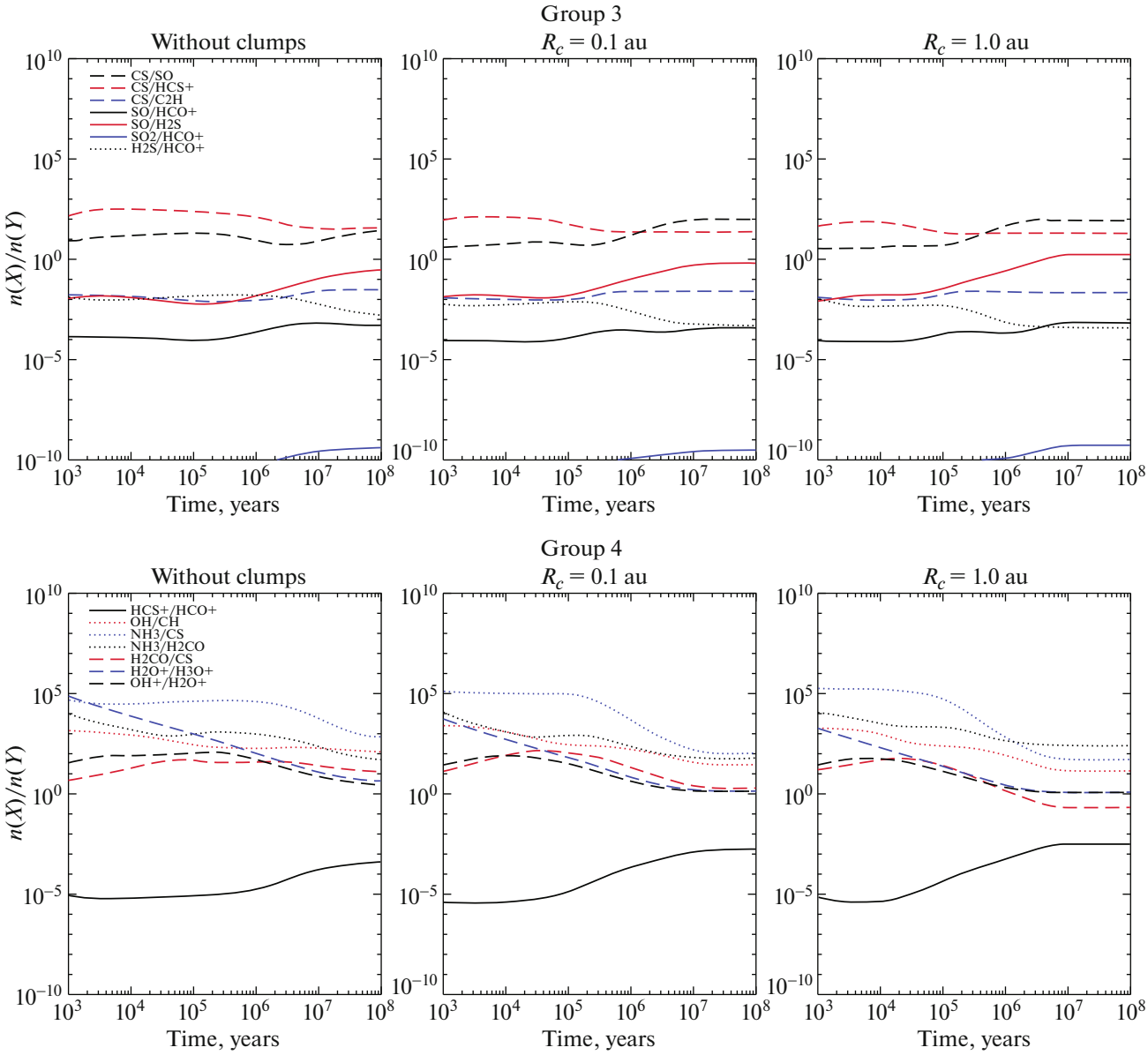


**Fig. 5.** Time dependent change of ratios of molecular abundances for different models of the diffuse cloud: the model without clumps (on the left panels), with clumps of radius of 0.1 au (on the central panels), with clumps of radius of 1.0 au (on the right panels). Evolution time from $10^3$ to $10^8$ years. Group 3 (upper row) and Group 4 (lower row) of molecules.

atomic form in, respectively, the models with and without clumps. The molecular hydrogen is important for the formation of simple molecules from Group 1, and it can be illustrated by the following reactions chain (Group 1 molecules are in bold):

$$C^+ + H_2 \rightarrow CH_2^+ + h\nu, \quad (1)$$

$$CH_2^+ + H_2 \rightarrow CH_3^+ + H, \quad (2)$$

$$CH_3^+ + e^- \rightarrow \mathbf{CH_2} + H, \quad (3)$$

$$\rightarrow \mathbf{CH_3} + h\nu, \quad (4)$$

$$\rightarrow \mathbf{CH} + H + H \quad (5)$$

and the following reactions,

$$C^+ + CH \rightarrow C_2^+ + H, \quad (6)$$

$$C_2^+ + H_2 \rightarrow C_2H^+ + H, \quad (7)$$

$$C_2H^+ + H_2 \rightarrow C_2H_2^+ + H, \quad (8)$$

$$C_2H_2^+ + e^- \rightarrow \mathbf{C_2H} + H, \quad (9)$$

$$\rightarrow \mathbf{C_2} + H + H. \quad (10)$$

Oxygen-bearing molecules form via similar reaction chains initiated by the highly active $H_3^+$ ion that forms

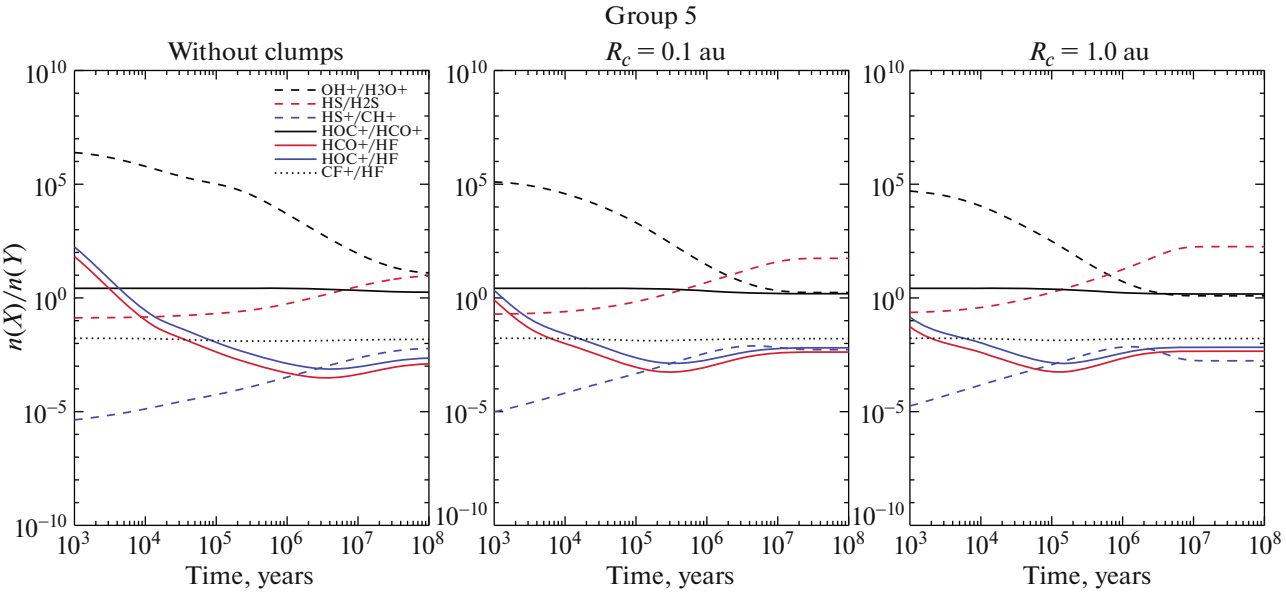


**Fig. 6.** Time dependent change of ratios of molecular abundances for different models of the diffuse cloud: the model without clumps (on the left panels), with clumps of radius of 0.1 au (on the central panels), with clumps of radius of 1.0 au (on the right panels). Evolution time from $10^3$ to $10^8$ years. Group 5 of molecules.

from the molecular hydrogen as a result of interaction with cosmic rays:

$$H_2 + \mathrm{CRP} \rightarrow H_2^+ + e^-, \quad (11)$$

$$H_2^+ + e^- \rightarrow H_3^+ + H, \quad (12)$$

$$H_3^+ + O \rightarrow OH^+ + H_2, \quad (13)$$

$$OH^+ + H_2 \rightarrow H_2O^+ + H, \quad (14)$$

$$H_2O^+ + H_2 \rightarrow H_3O^+ + H, \quad (15)$$

$$H_3O^+ + e^- \rightarrow \mathbf{OH} + H + H, \quad (16)$$

$$C^+ + OH \rightarrow CO^+ + H, \quad (17)$$

$$CO^+ + H_2 \rightarrow \mathbf{HCO} + H. \quad (18)$$

Finally, complex molecules form from the simpler ones. For example:

$$CH_3 + O \rightarrow \mathbf{H_2CO} + H. \quad (19)$$

We suppose that the reactions given above sufficiently illustrate the importance of $H_2$ molecule for the chemistry of simple compounds, therefore, for brevity we do not give similar reaction chains for other molecules.

Group 2 (lower row in Fig. 1) of molecules includes simple nitrogen-bearing molecules. The presence of gas-dust clumps in the model almost does not affect abundances of these molecules in comparison with molecules from Group 1. This is related to features of the chemistry of simple nitrogen-bearing molecules. In particular, $NH^+$, NH, $NH_2$, and $NH_3$ molecules form in the same chain of ion-molecule reactions and dissociative recombination reactions:

$$NH_i^+ + H_2 \rightarrow NH_{(i+1)}^+ + H, \quad i = 0\ldots3, \quad (20)$$

$$NH_{(i+1)}^+ + e^- \rightarrow NH_i, \quad i = 0\ldots3. \quad (21)$$

Wherein the first ion of the chain, $N^+$, is formed by cosmic-ray ionization of atomic nitrogen N already presented in the model. The rate of this process does not depend on the presence or absence of compact gas-dust clumps in our model, and that explains the independence of abundances of the listed simple nitrogen-bearing molecules from the presence or absence of clumps. The rates of the given reactions for the listed Group 2 molecules are limited by the abundance of nitrogen ions but not by the molecular hydrogen abundance. A similar discussion is valid for the other molecules of Group 2 but one should note the case of CN molecule. In order to explain the independence of abundance of this molecule on the presence of clumps, one need to take into account an increased rate of photodissociation due to lower opacity of the diffuse cloud with clumps in comparison the cloud without clumps. The increased rate of CN destruction in the model with clumps is compensated by the increased rate of its formation in reactions between atomic nitrogen and $C_2$ and CH molecules.

Group 3 of molecules contains sulfur-bearing molecules. The abundances of the following four molecules from this group in the models with clumps increase significantly in comparison with the model

without clumps: HS, CS, NS, and SO. As in the case of Group 1 molecules, the increase of abundances of these four molecules in the models with clumps is also due to the increased fraction of molecular hydrogen in the gas phase during the late times of the chemical cloud evolution in comparison with the model without clumps:

$$S^+ + H_2 \rightarrow H_2S^+ + h\nu, \quad (22)$$

$$H_2S^+ + e^- \rightarrow \mathbf{HS}, \quad (23)$$

$$HS + N \rightarrow \mathbf{NS} + H, \quad (24)$$

$$HS + O \rightarrow \mathbf{SO} + H. \quad (25)$$

CS molecule is formed by the dissociative recombination of $HCS^+$ ion, which also forms in ion-molecule reactions involving molecular hydrogen. It is interesting, that despite the fact that the CS and HS abundances relative to hydrogen in the models with clumps reach values of $10^{-11}$, we still can not explain the observed abundances of these molecules which are higher by approximately two orders of magnitude than the model ones.

Group 4 of molecules includes phosphorus-bearing and fluorine-bearing molecules. Unfortunately, our model includes only the basic chemistry of these types of compounds, and, as can be seen in Fig. 2, there are no significant differences in abundances of these molecules between the models with and without clumps. Therefore, we do not analyze features of their formation in this work.

Group 5 of molecules represents complex organics and associated ions. Methanol is the only one molecule in this group that reaches the maximum relative abundance of $10^{-11}$ that is high enough for the detection in observations. It is interesting, that this abundance is achieved in the model with clumps of sizes of 0.1 au. In both the models without clumps and with clumps of sizes of 1.0 au, the maximum methanol abundance is less by one order of magnitude. Such a behavior of methanol can be explained by the formation of methanol in the CO hydrogenation reactions on the surface of dust particles. The accretion rate of atoms and molecules from gas to dust surface in the models with clumps is higher than in the model without clumps. This increases the rate of methanol formation. On the other hand, the extinction of external radiation within the diffuse cloud in models with clumps is lower than in the model without clumps. Therefore, the rate of methanol destruction by ultraviolet photons is higher. In the model with clumps having the size of 0.1 au, the balance between formation and destruction of methanol is shifted in favor of formation and, thus, the methanol abundance becomes the highest one among all three diffuse cloud models. In the model with clumps with size of 1.0 au, the balance is that the resulting maximum methanol abundance is the same as in the model without clumps.

Group 6 of molecules includes molecules which are chemically dissimilar. One can see in Fig. 3 that abundances of most molecules in this group almost the same in the models with and without clumps. The exceptions are two important molecules, $H_2$ and $C_3$, whose abundances are higher in the models with clumps than in the model without clumps. In the model with clumps of different sizes, the formation of molecular hydrogen on the surface of dust particles is faster than in the model without clumps, and self-shielding "protects" $H_2$ from rapid destruction in more transparent diffuse cloud with clumps. Therefore, the formation of molecular hydrogen from atomic hydrogen is faster by an order of magnitude than in the model without clumps [12]. Formation of $C_3$ molecule in all models occurs due to the dissociative recombination reaction of $C_3H^+$ ion, which in turn is formed in the reaction with molecular hydrogen:

$$C^+ + C_2H \rightarrow C_3^+ + H, \quad (26)$$

$$C_3^+ + H_2 \rightarrow C_3H^+ + H, \quad (27)$$

$$C_3H^+ + e- \rightarrow C_3 + H. \quad (28)$$

It can be noted, that formation of $C_3$ molecule is turned out to be closely related to the abundance of molecular hydrogen in the medium in two chain stages at once: firstly, at the moment of $C_3H^+$ ion formation and, secondly, during the $C_2H$ molecule formation (in more detail its formation is described in the discussion of the chemical evolution of molecules from Group 1). The $C_3$ molecular abundances in the models with clumps approach the observed values, however they are still lower by approximately one and a half orders of magnitude than the observed values (see Table 4). $C_3$ molecule is ubiquitous in observations of the diffuse medium along various lines of sight [37]. This can indicate that this molecule is efficiently formed under the wide range of physical conditions characteristic for both relatively dense "translucent" clouds and diffuse molecular clouds considered in this work. In this case, the high values of abundance of this molecule in a diffuse cloud, which is characterized by low values of $A_V$, can be an indicator of the possible existence of compact dust-dust clumps in the cloud.

Results described above show that compact gas-dust clouds (clumps) with sizes of 0.1–1.0 au, which possibly can be formed in the interstellar medium as described in [10], have a limited effect on the chemical evolution of molecules and ions observed along the line of sight towards the diffuse interstellar clouds. Even though the abundances of some molecules in the models with clumps can increase by several orders of magnitude, they do not approach abundance values obtained from observations. The observed values are still higher than the model ones by 2–3 orders of magnitude. As the key factor which affects chemistry in the diffuse and translucent clouds is the opacity of cloud

(or visual extinction), we performed test calculations with the same parameters as for the model without clumps considered in this work but with $A_V = 2$ and $3^m$. The results of these calculations show that the increase of $A_V$ values has the significantly greater effect on molecular abundances than the presence of clumps in the model, and the significantly larger amount of compounds have better agreement between the model and observed abundances. Based on this fact we can conclude that high abundances of a number of molecules observed along the line of sights toward the diffuse clouds are actually achieved not in the diffuse gas itself (which is characterized by low density and $A_V < 1$), but most likely in the regions with denser gas, located on the line of sight and surrounded by the diffuse gas. This conclusion is consistent with several other studies of the molecular composition of the diffuse interstellar clouds ([3] and references therein).

Thus, according to the obtained results, the following main conclusions can be made:

1. The inclusion of the compact gas-dust clouds (clumps) into astrochemical models of the diffuse molecular cloud leads to an increase in the model abundances of a number of molecules in comparison with the values obtained in the standard model of the diffuse cloud, which assumes the homogeneous spatial distribution of dust and gas. However, the increased model abundances generally remain lower by 2–3 orders of magnitude than the molecular abundances obtained from observations of the diffuse clouds.

2. The diffuse cloud models with clumps with radii of 0.1 and 1.0 au allow one to explain $C_2H/HCO^+$, $HCN/C_2H$, CS/HCN, and OH/CH abundances ratios. At the same time, in all three diffuse cloud models with and without clumps, there are abundance ratios that are equally bad in terms of matching the observed values ($C_4H/C_2H$, $HC_3N/HCN$, and $SO_2/HCO^+$). However, in the model with 1 au clumps, these ratios become higher and somewhat more closer to the observational data than in the case of models with smaller clumps or without clumps. For a more accurate analysis of impact of the new model on the chemical evolution of specific molecules, one should make the simulations of the diffuse clouds with parameters corresponding to those objects where these molecules have been detected. This is an interesting task for the following studies.

3. We performed the test calculations of models that are completely similar to the diffuse cloud model without clumps but with the visual extinction values $A_V = 2$ and $3^m$. It was found, that the increase of $A_V$ values affects chemistry more than the inclusion of clumps in the model, and allows one to reproduce a greater number of observed molecular abundances, but not all of them. This result confirms assumptions made by a number of authors that the high abundances of some molecules in the diffuse medium can not be explained by the model of the diffuse cloud itself, which is characterized by low gas density and $A_V$, and that the high observed abundances of some molecules along the line of sight toward diffuse clouds arise in the regions of denser and less transparent (translucent) gas.

4. Nevertheless, clumps can be responsible for higher molecular abundances because they speed up the $H \rightarrow H_2$ transition by an order of magnitude and contribute to the faster formation of denser translucent regions.

## ACKNOWLEDGMENTS

The authors thank A.V. Ivlev for valuable discussions during the course of this work. The reported study was funded by RFBR according to the research project 18-32-00645. Work of S. Parfenov was made with the financial sup-port of Ministry of Science and Higher Education of the Russian Federation, project FEUZ-2020-0030. V. Sokolova and A. Vasyunin are members of the Max Planck Partner Group at the Ural Federal University

## REFERENCES

1. D. H. Wooden, S. B. Charnley, and P. Ehrenfreund, in *Composition and Evolution of Interstellar Louds,* Ed. by M. C. Festou, H. U. Keller, and H. A. Weaver (Univ. of Arizona Press, Tucson, 2004), p. 33.
2. A. G. G. M. Tielens, *The Physics and Chemistry of the Interstellar Medium* (Cambridge Univ. Press, New York, 2005).
3. T. P. Snow and B. J. McCall, Ann. Rev. Astron. Astrophys. **44**, 367 (2006).
4. R. Lucas and H. S. Liszt, Astron. Astrophys. **358**, 1069 (2000).
5. H. Liszt and R. Lucas, Astron. Astrophys. **370**, 576 (2001).
6. R. Lucas and H. S. Liszt, Astron. Astrophys. **384**, 1054 (2002).
7. D. A. Neufeld, B. Godard, M. Gerin, G. Pineau des Forets, et al., Astron. Astrophys. **577**, A49 (2015).
8. M. Gerin, M. de Luca, J. Black, J. R. Goicoechea, et al., Astron. Astrophys. **518**, L110 (2010).
9. B. Godard, E. Falgarone, M. Gerin, and D. C. Lis, Astron. Astrophys. **540**, A87 (2012).
10. V. N. Tsytovich, A. V. Ivlev, A. Burkert, and G. E. Morfill, Astrophys J. **780**, 131 (2014).
11. A. B. Ostrovskii et al., Mon. Not. R. Astron. Soc. **495** (4), 4314 (2020). https://doi.org/10.1093/mnras/staa1460
12. A. V. Ivlev, A. Burkert, A. Vasyunin, and P. Caselli, Astrophys J. **861**, 30 (2018); arXiv:1805.1179.
13. G. Morfill, Plasma Phys. Rep. **26**, 682 (2000). https://doi.org/10.1134/1.1306997
14. R. Bingham and V. N. Tsytovich, Astron. Astrophys. **376**, L43 (2001).
15. V. N. Tsytovich and K. Watanabe, Contrib. Plasma Phys. **43** (2), 51 (2003). https://doi.org/10.1002/ctpp.200310006

16. S. A. Khrapak, A. V. Ivlev, and G. Morfill, Phys. Rev. E **64**, 046403 (2001).
17. A. I. Vasyunin and E. Herbst, Astrophys J. **769**, 34 (2013).
18. R. T. Garrod and E. Herbst, Astron. Astrophys. **457**, 927 (2006); astro-ph/0607560.
19. V. A. Sokolova, A. B. Ostrovskii, and A. I. Vasyunin, Astron. Rep. **61**, 678 (2017).
20. M. Asplund, N. Grevesse, and A. J. Sauval, Nucl. Phys. A **777**, 1 (2006). http://www.sciencedirect.com/science/article/pii/S0375947405009541
21. S. Yamamoto, *Introduction to Astrochemistry. Chemical Evolution from Interstellar Clouds to Star and Planet Formation* (Springer, Tokyo, Japan, 2017).
22. N. Indriolo and B. J. McCall, Astrophys J. **745**, 91 (2012).
23. A. I. Vasyunin, A. M. Sobolev, D. S. Wiebe, and D. A. Semenov, Astron. Lett. **30**, 566 (2004); astro-ph/0311450.
24. J. C. Laas and P. Caselli, Astron. Astrophys. **624**, A108 (2019). https://doi.org/10.1051/0004-6361/201834446
25. J. Chantzos, V. M. Rivilla, A. Vasyunin, E. Redaelli, L. Bizzocchi, F. Fontani, and P. Caselli, Astron. Astrophys. **633**, A54 (2020); arXiv: 1910.13449.
26. V. Thiel, A. Belloche, K. M. Menten, R. T. Garrod, and H. S. P. Muller, Astron. Astrophys. **605**, L6 (2017). https://doi.org/10.1051/0004-6361/201731495
27. H. Liszt and R. Lucas, Astron. Astrophys. **391**, 693 (2002).
28. H. S. Liszt, R. Lucas, and J. Pety, Astron. Astrophys. **448**, 253 (2006).
29. P. Crane, D. Lambert, and Y. Sheffer, Astrophys. J. Suppl. **99**, 107 (1995).
30. M. Gerin, M. Luca, J. Goicoechea, E. Herbst, et al., Astron. Astrophys. **521**, L16 (2010).
31. K. M. Menten, F. Wyrowski, A. Belloche, R. Güsten, L. Dedes, and H. S. P. Müller, Astron. Astrophys. **525**, A77 (2011).
32. D. A. Neufeld, E. Falgarone, M. Gerin, and B. Godard, Astron. Astrophys. **542**, L6 (2012).
33. J. F. Corby, B. A. McGuire, E. Herbst, and A. J. Remijan, Astron. Astrophys. **610**, A10 (2018). https://doi.org/10.1051/0004-6361/201730988
34. M. Gerin, D. A. Neufeld, and J. R. Goicoechea, Ann. Rev. Astron. Astrophys. **54**, 181 (2016).
35. H. Liszt, M. Gerin, A. Beasley, and J. Pety, Astrophys. J. **856,** 151 (2018). https://doi.org/10.3847%2F1538-4357%2Faab208
36. M. Gerin, H. Liszt, D. Neufeld, B. Godard, P. Sonnentrucker, J. Pety, and E. Roueff, Astron. Astrophys. **622**, A26 (2019). https://doi.org/10.1051/0004-6361/201833661
37. T. Oka, J. Dahlstrom, B. McCall, S. Friedman, L. Hobbs, P. Sonnentrucker, D. Welty, and D. York, Astrophys. J. **582**, 823 (2008).